PHYSICAL REVIEW B VOLUME 28, NUMBER 12 15 DECEMBER 1983

High-pressure Raman study of zone-center phonons in $PbTiO_3$

J. A. Sanjurjo* and E. López-Cruz†
Max-Planck-Institut für Festkörperforschung, Heisenbergstrasse 1, D-7000 Stuttgart 80, Federal Republic of Germany

Gerald Burns
Max-Planck-Institut für Festkörperforschung, Heisenbergstrasse 1, D-7000 Stuttgart 80, Federal Republic of Germany and IBM Thomas J. Watson Research Center, Box 218, Yorktown Heights, New York 10598

(Received 15 August 1983)

A complete study of the $\vec{k}=\vec{0}$ optical phonons of the ferroelectric tetragonal $PbTiO_3$ as a function of hydrostatic pressure has been carried out using Raman spectroscopy. The coalescence, to the same frequency, of the high-energy [A_1(TO), E(TO)] pairs of phonons in the ferroelectric phase and the disappearance of the first-order Raman lines in the cubic phase has enabled us to determine the transition pressure P_c, as well as the second-order character of the phase transition. Our results also suggest the existence of a tricritical point in the (P,T) phase diagram. Using the Liddane-Sachs-Teller relation we calculate the static dielectric constant as a function of pressure and compare the results with previous dielectric measurements. Moreover, we discuss the soft phonons, their damping, and their behavior near the phase transition. It is found that the soft E(TO) phonon damping function is nearly constant over a wide frequency range and that it appears to diverge near the phase transition.

I. INTRODUCTION

For ferroelectric materials, T_c is defined as the transition temperature between the high-temperature paraelectric phase and the lower-temperature ferroelectric phase. For displacive ferroelectric transitions it has been found that T_c decreases with hydrostatic pressure.[1] Thus high-pressure studies of the phonon spectra in the ferroelectric phase of displacive ferroelectrics are of interest for several reasons.[2] First, by varying the pressure P, the high-pressure paraelectric phase can be reached at P_c. This enables one to determine the pressure dependence of the mode frequencies, to examine the spectra above P_c, and to compare the results with measurements made as a function of temperature T up to and above T_c. Second, the soft mode for displacive phase transition is usually particularly sensitive to pressure (and temperature) changes. In fact, for a second-order phase transition the soft-mode frequency ω_0 goes to zero at P_c (or T_c). For example, this enables one to measure the frequency dependence of the damping constant γ of the soft mode(s) over a very wide frequency range, i.e., it determines $\gamma(\omega)$. Also, the mode pairs in the ferroelectric phase originating from the same parent, triply degenerate mode in the paraelectric phase can be studied.

In this paper we discuss our high-pressure Raman results on the phonon frequencies in the ferroelectric $PbTiO_3$. We have been able to measure the frequencies of the phonon modes up to P_c and thus, besides discussing the points just mentioned, we compare our results with those obtained by Burns and Scott[3] up to T_c at atmospheric pressure. A brief article on our results on $\gamma(\omega)$ has already been published.[4]

II. EXPERIMENTAL DETAILS

$PbTiO_3$ crystals were grown from PbO flux[3] and polished to 30 μm thickness. A small piece, suitable to fit the 200-μm hole of the pressure cell gasket, was chosen under the microscope. A gasketed diamond anvil cell, similar to the one described by Syassen and Holzapfel,[5] was employed for the Raman measurements. A 16:3:1 methanol-ethanol-water mixture served as the pressure transmitting medium,[6] and the fluorescence of a small ruby chip placed near the sample was used for the pressure calibration.[7] Backscattering geometry ($\sim 30°$ angle of incidence outside the cell) was used along with an Ar^+-ion laser (5145-Å line), a Spex model-1401 spectrometer with and without a third monochromator, and a standard photon counting technique. This setup, with a 20-μm-split aperture, was necessary to reduce background light so that the soft E(TO) and A_1(TO) phonons could be studied at very low energies. All measurements were carried out at room temperature ($\simeq 25\,°C$), and the accuracy of the pressures is ± 0.1 GPa.

III. RESULTS

$PbTiO_3$ belongs to the O_h^1 ($Pm3m$) space group, with one formula unit per primitive cell, in the cubic (paraelectric) phase. Thus there are 12 optic modes at the Γ point of the Brillouin zone. The optic modes transform as the $3T_{1u}+T_{2u}$ irreducible representation of the O_h point group. The T_{1u} modes are infrared active and T_{2u} is the so-called "silent mode" since it is neither infrared nor Raman active.

In the ferroelectric tetragonal phase [C_{4v}^1 ($P4mm$) space group] each triply degenerate T_{1u} mode splits into two modes transforming as the A_1+E irreducible representation of the C_{4v} point group. The silent mode also, in principle, splits into B_1+E modes that are Raman active; however, the separation between these two modes cannot be measured, so that the single feature that one measures for these phonons is called B_1+E.

However, because of the long-range electrostatic forces, the situation for the T_{1u} modes (in the cubic phase) and the A_1+E modes (in the tetragonal phase) that arise from the T_{1u} modes is more complicated. Each of these optic modes can have a polarization transverse to the direction of propagation (TO mode) as well as polarization along the direction of propagation (LO mode). We follow the straightforward labeling scheme used earlier,[3] and, ignoring the B_1+E feature, the following modes should be observable in the tetragonal ferroelectric phase:

A_1(3TO)	A_1(3LO)	E(3TO)	E(3LO)
A_1(2TO)	A_1(2LO)	E(2TO)	E(2LO)
A_1(1TO)	A_1(1LO)	E(1TO)	E(1LO)

where the numbers 1, 2, and 3 are used merely as a method for labeling those modes. For each series, 1 refers to the lowest-frequency phonon and 3 refers to the highest-frequency phonon. The very lowest-frequency modes are E(1TO) and A_1(1TO), which are the "soft modes" in that they tend to zero frequency as T_c or P_c is approached from below. (Note that for one crystal orientation only 12 optic modes occur.) These modes "connect" to the soft T_{1u}(1TO) mode of the cubic phase.

A. High-frequency modes (and P_c)

In this section we discuss the results of the high-frequency modes, i.e., all of the modes excluding the E(1TO) and A_1(1TO). In contrast to the measurements as a function of temperature,[3] where large single crystals and right-angle Raman scattering were used and all of the modes were reported, we could not observe all of the modes in our pressure cell. However, all the TO modes were observed, and typically these have the largest pressure (and temperature) dependence.

Figure 1 shows typical experimental data at several pressures and Fig. 2 gives the frequencies versus pressure. As can be seen, our data are in good agreement with the results of Cerdeira *et al.*,[8] who measured the modes to approximately 6.6 GPa.

It is important to determine P_c from the high-energy modes because even if the phase transition is first order, we expect the soft modes to have very small frequency shifts near P_c, and because of the damping they should be very difficult to observe. Further, from the dielectric data of Samara[9] at 3.4 GPa, it is suggested that, at room temperature, the phase transition tends toward being a second-order transition when P_c is reached.

From the high-energy modes we have determined P_c by two approaches. First, at P_c we observe that the first-order Raman modes disappear abruptly. This is expected since in the cubic phase the normal modes of vibration

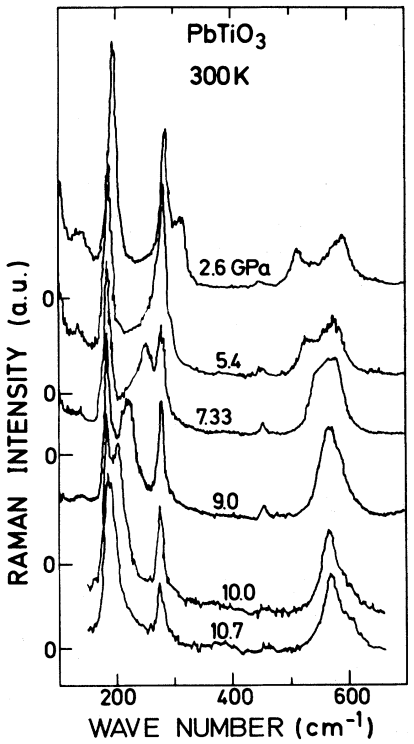

FIG. 1. Typical Raman spectra of the high-frequency modes at various pressures.

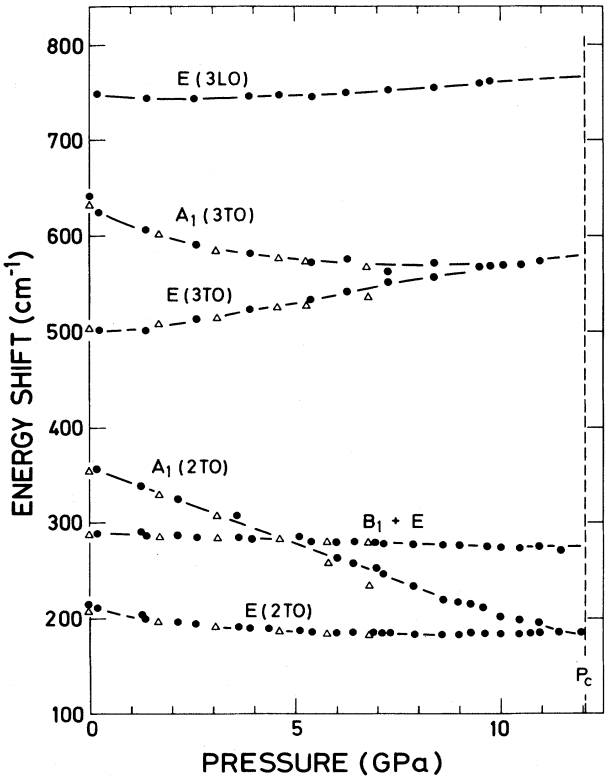

FIG. 2. Position of the Raman peaks as a function of pressure for the high-frequency phonons. The open triangles are data taken from Cerdeira *et al.* (Ref. 8) and the dashed lines are visual guides.

transform as the $3T_{1u}+T_{2u}$ irreducible representations of the O_h point group and are thus not Raman active. Second, in the same pressure range we observe that the appropriate $A_1(2TO)+E(2TO)$ as well as the $A_1(3TO)+E(3TO)$ pairs of modes coalesce to the same frequency (see Fig. 2). These pairs come from their "parent" $T_{1u}(2TO)$ and $T_{1u}(3TO)$ modes, respectively. It is only for a second-order phase transition that we expect to find the coalescence observed in the figure. Thus we find that $P_c=12.1\pm0.2$ GPa, and we also determine that the transition is second order.

We should discuss the Raman data above P_c in somewhat more detail because of the long-standing controversy over the broad spectra observed in the cubic phase of $BaTiO_3$ and $KNbO_3$ above T_c and/or P_c. In $PbTiO_3$ above T_c no Raman intensity was observed,[3] as expected from the selection rules. Similarly, as a function of pressure we find that the modes disappear at P_c and that no Raman intensity is observed at higher pressures. Thus $PbTiO_3$ behaves as expected. Actually, for $BaTiO_3$ at T_c all of the $3A_1+3E$ modes as well as the B_1+E "silent" mode also disappear. However, in $BaTiO_3$ one is left with some strong, broad features that are still, to this day, unexplained. Nevertheless, these features are not observed in $PbTiO_3$.

B. Soft-mode frequencies

Figure 3 shows some of the typical (0—100 cm^{-1}) Stokes-Raman spectra of the soft-phonon modes at fairly high pressures. The lowest mode is the $E(1TO)$ mode and the higher one is $A_1(1TO)$. The latter mode is not observable at atmospheric pressures,[3] but it is easily observable for pressures above 1 GPa. Note that the $A_1(1TO)$ mode is fairly broad even at low pressures, whereas the $E(1TO)$ mode is much narrower. The signal-to-noise ratio (S/N) is very large, the noise being no larger than the width of the ink lines in Fig. 3. It is not the S/N that limits our observations at high pressure, i.e., small energy shift, but rather the Rayleigh scattering. Even so, as can be seen, useful data down to 12 cm^{-1} have been obtained. It is our very large S/N, very large stray light rejection, as well as much higher pressures that distinguish our measurements from the previous high-pressure work,[8] and all three of these ingredients are critical for obtaining the soft-mode data presented here. As can also be seen in Fig. 3, above 11.4 GPa we no longer can resolve a peak in the spectra. We have only used quantitatively the data obtained at lower pressures. Thus all of the results in the soft modes come from underdamped spectra.

For lower pressures the two soft modes are well separated; particularly, the $E(1TO)$ mode is very underdamped so that we can take the frequencies from the peaks in the spectra. However, at higher pressures the damping of the modes increases (discussed below) and the two soft modes begin to overlap each other (see Fig. 3) so that a computer-fitting procedure was used. We have made a least-squares fit with two Lorentzian functions

$$I(\omega)=[n(\omega)+1]\sum_{i=1}^{2}\frac{F_i\omega_{0i}^2\gamma_i\omega}{(\omega_{0i}^2-\omega^2)^2+\gamma_i^2\omega^2}\ , \tag{1}$$

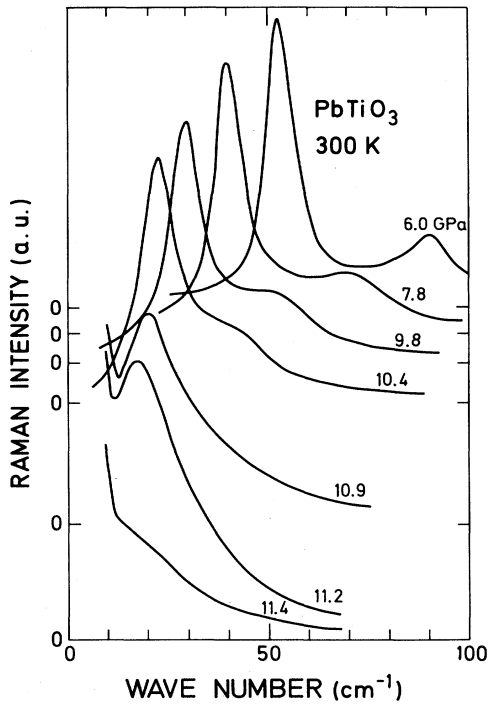

FIG. 3. Raman spectra of the soft phonons at various pressures.

where $i=1$ and 2 correspond to the $E(1TO)$ and $A_1(1TO)$ modes, respectively, and F_i, ω_{0i}, and γ_i are the scale factor, mode frequency, and linewidth of the two phonons. The parameters are in excellent agreement with those taken from the peak positions and the full width at half maximum intensity at lower pressures. The fits are very good, using, at a single pressure, a frequency-independent damping constant for each of the soft modes. Figure 4 shows the results of the fitting using Eq. (1) so that the two soft modes are seen separately. The fact that the $A_1(1TO)$ mode is considerably wider than the $E(1TO)$ mode is made clear.

In Fig. 5 we plot the square of the frequencies of the two soft modes versus pressure (along with their γ's, to be discussed below). Especially at higher pressures the data show straight-line behavior of ω^2 vs P, indicating a Curie-Weiss pressure law. The solid lines represent the soft-phonon frequencies and are given by

$$\omega_{TO}^2=\Omega_0^2(1-P/P_c)\ , \tag{2}$$

where $P_c=12.1$ GPa, and $\Omega_0=72.5$ cm^{-1} and 123 cm^{-1} for the $E(1TO)$ and $A_1(1TO)$ modes, respectively. [The dashed line is a guide to the eye for helping one follow the results for the pressure dependence of the damping constant of the $E(1TO)$ mode, to be discussed below.]

C. Soft-mode damping

Also shown in Figs. 5 and 6 is the damping constant γ obtained via Eq. (1) for the $E(1TO)$ and $A_1(1TO)$ soft modes. As noted earlier, all of these results come from

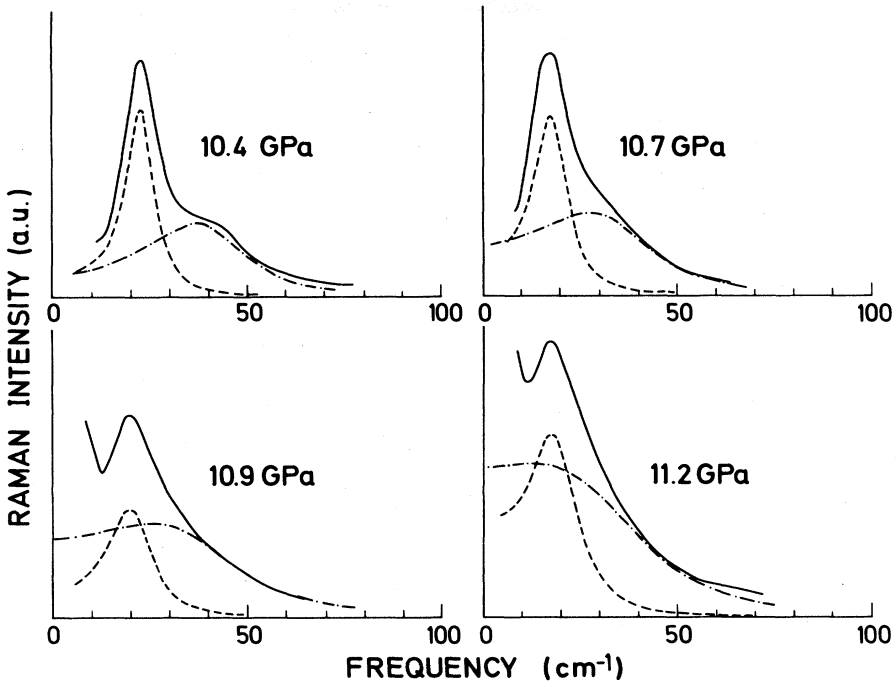

FIG. 4. Typical spectra of the soft phonons as a function of pressure. The dashed and dashed-dotted lines are the best-fit profiles of the E(1TO) and A_1(1TO) soft phonons using a Lorentzian response function.

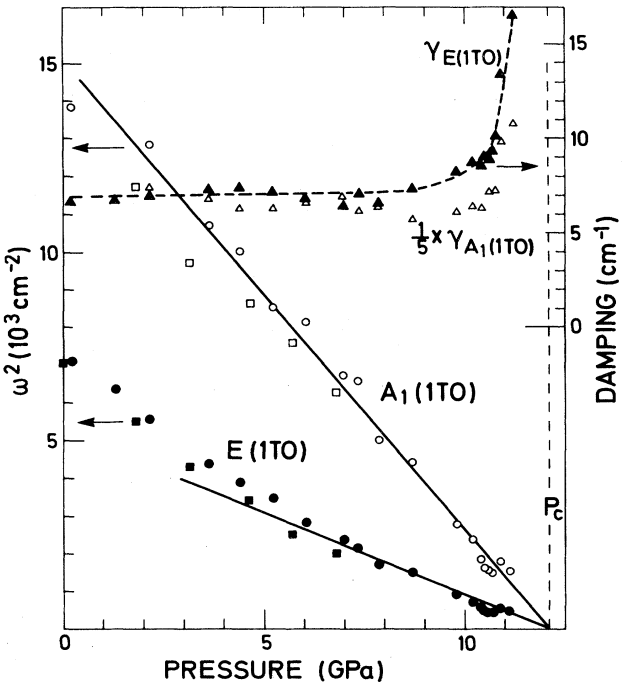

FIG. 5. Square of the frequency and damping constant as a function of pressure for the E(1TO) (full solid circles and triangles) and for the A_1(TO) (open circles and triangles) soft phonons. The squares are data from Ref. 8. The solid lines are least-squares fittings with Eq. (2).

underdamped modes. Also note that over most of the pressure range the E and A_1 soft modes are well separated (Fig. 3) so that there is little interference. However, above $P \simeq 10.9$ GPa the two soft modes are close in frequency and the broad A_1(1TO) mode tends to act as a base line for the much narrower E(1TO) mode (see Fig. 4).

Over most of the pressure range, γ is independent of pressure. However, near P_c it increases sharply. This will be discussed below.

IV. DISCUSSION

A. High-frequency modes

We have fitted the pressure dependence of the high-frequency phonons, as well as the low-pressure region of the soft A_1(TO) and E(TO) phonons, using a linear regression (see Figs. 2 and 6), with the exception of the A_1(3TO) mode for which we have used a second-order polynomial. The linear coefficients were used to calculate the mode-Grüneisen parameters

$$\eta \equiv -\left[\frac{d\ln\omega}{d\ln v}\right]_{P=0} = \frac{B_T}{\omega_0}\left[\frac{d\omega}{dP}\right]_{P=0}, \tag{3}$$

where ω_0 is the frequency of the mode at $P=0$, and $B_T = 85.7$ GPa is the isothermal bulk modulus.[8] In Table I these parameters are listed together with the ones obtained by Cerdeira *et al.*[8] The concordance is good with the exception of A_1(2TO) and E(2TO) for which we have almost a linear pressure dependence, but in Ref. 8 a parabolic fit was used. Samara[9] has related the mode-Grüneisen parameter of the soft mode in the paraelectric

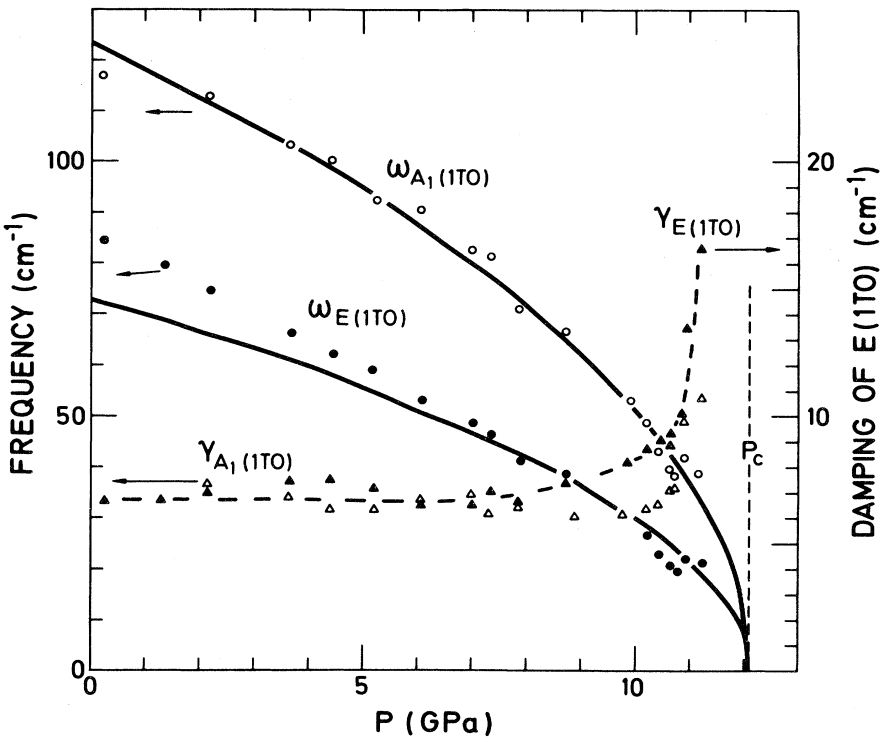

FIG. 6. Frequency and damping constant as a function of pressure for the E(1TO) (solid circles and triangles) and for A_1(1TO) (open circles and triangles) soft phonons. The solid lines are calculated using Eq. (2).

phase with quantities obtained from dielectric measurements:

$$\eta_S = \frac{B_T \epsilon}{2C^*} , \tag{4}$$

where ϵ is the dielectric constant and C^* is the Curie-Weiss constant. The above relation can be used in the ferroelectric side of a second-order phase transition. Using the Curie-Weiss law for the dielectric constant [$\epsilon = C^*/(P - P_c)$], Eq. (4) yields

$$\eta_S = -B_T/2P_c \tag{5}$$

at $P = 0$ GPa. Equation (5) can also be obtained directly from Eqs. (2) and (3). Cerdeira *et al.*[8] have used Eq. (5) to calculate the mode-Grüneisen parameter of the soft E(TO) phonon. They have used the value of $P_c = 7.6$ GPa extrapolated from Samara's data,[9] and they have obtained the value $\eta_S = -5.9$, in very good agreement with the experimental value (see Table I). Using the actual value of $P_c = 12.1$ GPa, Eq. (5) yields $\eta_S = -3.5$, substantially lower than the experimental value. This is due to the fact that the E(1TO) frequencies deviate from the mean-field expression [Eq. (2)] (at lower pressures), as can be seen in Fig. 6. Equation (5) holds also for the A_1(1TO) soft pho-

TABLE I. Parameters obtained from a least-squares fit of the pressure dependence of the phonon frequencies.

Mode	$d\omega/dP$[a] (cm^{-1}/GPa)	$d\omega/dP$[b] (cm^{-1}/GPa)	Mode-Grüneisen parameter η[a]	η[b]
E(1TO)	−5.8 ±0.2	−6 ±0.2	−5.8 ±0.2	−6.0 ±0.2
A_1(1TO)	−6.97±0.5	−5.5±0.5	−4.7	−4.0 ±0.5
E(2TO)	−2.3 ±1	−4.3±1	−0.98	−1.8 ±0.4
B_1+E	−1.38±0.4	−1.5±0.3	−0.41	−0.44±0.09
A_1(2TO)	−15.17±0.5	−11.5±0.8	−3.66	−2.8 ±0.2
E(3TO)	7.14±1	4.9±0.5	1.21	0.84±0.08
A_1(3TO)	−16.9 ±2	−24.0±2	−2.26	−3.2 ±0.3
E(3LO)	1.36±0.5		0.08	

[a]This work.
[b]See Ref. 8.

non, but in this case the agreement is good if we compare it to the experimental value found in Table I ($\eta_S=-4.7$). This is consistent with Fig. 6, where it can be seen that the A_1(1TO) phonon obeys Eq. (2) in the low-pressure range.

B. Soft-mode frequencies

In the right-angle Raman measurements as a function of temperature by Burns and Scott,[3] all of the phonons were observed. Thus, using the Lyddane-Sachs-Teller (LST) relationship

$$\frac{\epsilon(0)}{\epsilon_\infty}=\frac{\omega_{\mathrm{LO1}}^2}{\omega_{\mathrm{TO1}}^2}\frac{\omega_{\mathrm{LO2}}^2}{\omega_{\mathrm{TO2}}^2}\frac{\omega_{\mathrm{LO3}}^2}{\omega_{\mathrm{TO3}}^2}\ , \tag{6}$$

one can calculate, in a straightforward manner, $\epsilon(0)/\epsilon_\infty$. In this equation $\epsilon(0)$ is the clamped dielectric constant at zero frequency, ϵ_∞ is the square of the optic index of refraction extrapolated to well below the electronic resonances, and ω_{LO} and ω_{TO} refers to the LO and TO modes, where 1 refers to the soft mode as used through this paper. Of course, our measurements are in the tetragonal phase of $PbTiO_3$ where the dielectric constant along the ferroelectric c axis, $\epsilon(0)_c$, is determined by the frequencies of the A_1 modes, and the dielectric constant perpendicular to the c axis, $\epsilon(0)_a$, is determined by the frequencies of the E modes. Substituting into Eq. (6) the appropriate room-temperature values of the mode frequencies and using $\epsilon_\infty=6.37$, we obtain[3] $\epsilon(0)_c=41.1$ and $\epsilon(0)_a=106.7$. The soft phonons make the largest contribution to these dielectric constant values, and as T_c is approached their fractional contribution increases.[3]

We would like to perform a similar analysis for the pressure dependence of the dielectric constant. As shown in Fig. 2, although all of the TO modes have been measured, all of the LO modes have not been measured. However, first we notice that the LO modes vary less with temperature than do the TO modes.[3] Second, the E(3LO) mode varies more with temperature than do any of the other LO modes; yet, as a function of pressure, the E(3LO) mode varies very little (Fig. 2). Third, the soft-mode frequencies go to zero at P_c and are fairly low with a large-pressure dependence over the entire range so that they will dominate $\epsilon(0)$ at the onset. Thus, to calculate $\epsilon(0)$ we have assumed that that pressure dependence of the LO modes can be neglected. Then the pressure dependence of $\epsilon(0)_c$ and $\epsilon(0)_a$ can be determined via Eq. (6) using the mode frequencies in Figs. 2 and 6. The results are shown in Fig. 7. In the high-pressure region the dielectric constant can be approximated by

$$\epsilon(0)/\epsilon_\infty=C'/(P_c-P)\ , \tag{7}$$

where C' is calculated using the LO phonon frequencies of Ref. 3, the extrapolated values of the high-frequency TO modes at P_c (see Fig. 2) and Eq. (2). We obtain $C'=3.0\times10^3$ GPa for the $\epsilon(0)_a$ (determined by the E modes) and $C'=2.4\times10^3$ GPa for the $\epsilon(0)_c$ (determined by the A_1 modes).

Using Eq. (4) and the values of C' obtained above, in Fig. 7 we plot $[\epsilon(0)/\epsilon_\infty]^{-1}=(P_c-P)/C'$. It can also be seen in this figure that $[\epsilon(0)_c/\epsilon_\infty]^{-1}$ deviates from a line

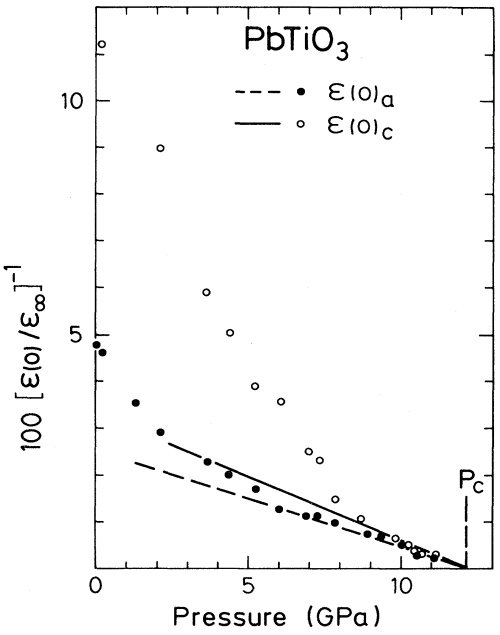

FIG. 7. Inverse of the static dielectric constant as a function of pressure, calculated using the LST relation [Eq. (6)]: solid circles, E-phonon contribution $\epsilon(0)_a$; open circles, A_1-phonon contribution $\epsilon(0)_c$. The continuous line $\epsilon(0)_c$ and the dashed line $\epsilon(0)_a$ are calculated as explained in the text.

in the low-pressure side due to the strong pressure variation of the A_1(2TO) and A_1(3TO) phonons.

In a second-order phase transition the dielectric constant along the ferroelectric axis $\epsilon(0)_c$, can be related to the dielectric constant in the paraelectric phase. In the cubic phase the $\epsilon(0)$ obeys the Curie-Weiss law $\epsilon(0)=C^*/(P-P_c)$. The Devonshire phenomenological theory predicts a Curie-Weiss law for the dielectric constant along the ferroelectric axis [Eq. (7)] with $C'=C^*/2$.[10] Our value of $C'=2.4\times10^3$ GPa is in good agreement with the Curie-Weiss constant obtained by Samara[9] ($C^*=4.5\times10^3$ GPa). This result is another indication of the second-order character of the phase transition.

C. Soft-mode damping

To analyze the behavior of the damping, we adopt the following point of view. By varying the pressure we can "tune" the soft mode from 88 to 0 cm^{-1} and observe the frequency dependence of the damping $\gamma(\omega)$. With this point of view, in Fig. 8, we plot γ of the E(1TO) mode as a function of the mode frequency ω_0. From the figure we see that $\gamma(\omega)$ of E(1TO) is essentially independent of ω between 88 and approximately 33 cm^{-1}. This is in disagreement with published room-temperature polariton results,[11] and these results have been discussed carefully.[4] Basically, since the pressure results are experimentally so straightforward to obtain, we believe that they are correct. However, to obtain $\gamma(\omega)$ from the polariton results requires computer deconvolution of the broad features and

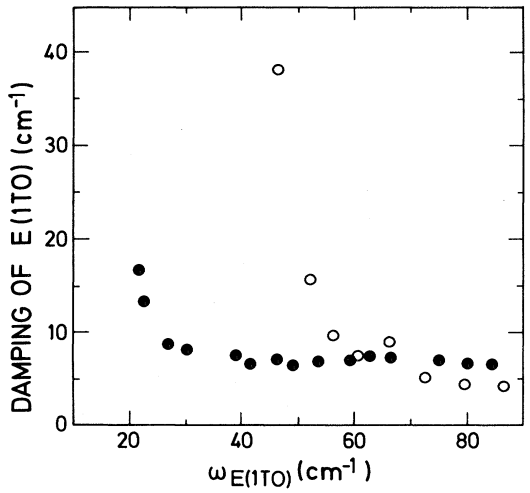

FIG. 8. γ vs ω for the soft E(1TO) phonon. The solid circles are our pressure results and the open circles are the polariton results (Ref. 11).

the assumption of no extraneous scattering from the sample.[4] The latter may be particularly troublesome when doing forward-scattering polariton measurements. Quite independent of the results for $\gamma(\omega)$ of the E(1TO) mode from Fig. 5 (or Fig. 2 in Ref. 4), we see that $\gamma(\omega)$ of the A_1(1TO) mode is also independent of ω between approximately 120 and 40 cm^{-1}. Thus, it seems clear that as long as one is not near P_c, γ is independent of ω over a wide frequency range. This is complementary to what is found from the high-temperature Raman results; near T_c the E(1TO) line is very broad (although underdamped). Yet over a range of 100 cm^{-1} it can be fitted extremely well with a frequency-independent damping constant.[3]

γ near P_c. Close to the phase transition at P_c, γ of the E(1TO) mode increases rapidly, as can be seen in Figs. 3—5 and 8. This occurs above approximately 10.5 GPa and is similar to the results for γ of E(1TO) as a function of temperature just below T_c for zero pressure.[3] For the temperature case, in the tetragonal phase this phonon is always underdamped and abruptly disappears above the first-order transition at T_c. As a function of pressure the transition is second order; hence ω_0 goes to zero. Naturally, this makes measurements of γ just below P_c difficult to obtain since the mode becomes overdamped. In a high-pressure cell the measurement problem is compounded by the scattering of the unshifted laser light by the diamond. Nevertheless, we have obtained data above approximately 12 cm^{-1} (Fig. 3) and have fitted the underdamped E(1TO) mode up to 11.2 GPa, which is the highest pressure for which we can obtain a peak for the E(1TO) mode. Thus, we again emphasize that singular behavior observed for γ below P_c is measured while the E(1TO) mode is *still underdamped.* It is improbable that this has anything to do with a particular frequency[11]; rather it appears to occur as the transition is approached (near P_c or T_c).

The γ of the soft A_1(1TO) mode also appears to diverge as P_c is approached (Fig. 5). However, in Figs. 3 and 4 it can be seen why we are less sure experimentally of this behavior because (a) the broader A_1(1TO) mode tends to appear as a "base line" under the sharper E(1TO) mode; and (b) near P_c, where γ of the A_1(1TO) appears to increase sharply, its frequency is very low and this base-line effect becomes accentuated, and above approximately 10.8 GPa we no longer see a distinct peak from this mode.

Since the behavior near P_c or T_c is anomalous, we discuss the origin of $\gamma(\omega)$. The temperature or pressure dependence of the soft-mode frequency as well as the frequency dependence of the damping can be accounted for by the anharmonic complex self-energy $\Sigma(\vec{q},\omega,T)=\Delta-i\Gamma$, where $\vec{q}$ is the phonon wave vector and T is the temperature.[12] The real part gives the renormalized soft-mode frequency ω_0 as $\omega_0^2=\Omega_0^2+2\Omega_0\Delta$, where Ω_0 is the pure harmonic frequency (ω_0 is what we actually measure as a function of T or P). The imaginary part is related to the phonon damping constant γ as $\Gamma=\omega\gamma/2\Omega_0$. For third-order anharmonic interaction Γ is expressed as[12]

$$\Gamma(\vec{q}jj',\Omega)=\frac{18\pi}{h^2}\sum_{\vec{q}_1,\vec{q}_2,j_1,j_2} V\begin{vmatrix}\vec{q} & -\vec{q}_1 & -\vec{q}_2\\ j & j_1 & j_2\end{vmatrix} \times V\begin{vmatrix}-\vec{q} & \vec{q}_1 & \vec{q}_2\\ j' & j_1 & j_2\end{vmatrix} S(\Omega)\,, \quad (8)$$

where

$$S(\Omega)=(\bar{n}_1+\bar{n}_2+1)[\delta(\omega_1+\omega_2-\Omega)-\delta(\omega_1+\omega_2+\Omega)] +(\bar{n}_2-\bar{n}_1)[\delta(\omega_1-\omega_2-\Omega)-\delta(\omega_1-\omega_2+\Omega)]\,, \quad (9)$$

where $\bar{n}_1$ and $\bar{n}_2$ are Bose-Einstein thermal factors. Equation (8) can be evaluated by summing over the whole Brillouin zone, knowing the matrix elements V. The resulting frequency dependence of the damping function Γ should reflect the structure of the two-phonon density of states:

$$\Gamma(\omega)\simeq 18\pi(n_1+n_2+1)\,|\,W_{\rm av}\,|^2\rho_2^+(\omega) +18\pi(n_1-n_2)\,|\,W'_{\rm av}\,|^2\rho_2^-(\omega)\,, \quad (10)$$

where $W_{\rm av}$ and $W'_{\rm av}$ are effective third-order interaction strengths and $\rho_2^+(\omega)$ and $\rho_2^-(\omega)$ are sum and difference combinations (two-phonon density of states), respectively. Normally, the strongest decay channel for zone-center TO phonons is in a combination of zone-boundary acoustic phonons. At constant temperature there are a few examples where one can vary ω_0 across a two-phonon density-of-states peak by means of hydrostatic pressure[13,14] or forward angle (polariton) scattering.[15] However, in these cases[13–15] $\Delta\omega_0/\omega_0$ is relatively small, but enough to see a variation in $\gamma(\omega)$.

In our case (see Figs. 6 and 8), the soft-mode linewidth is almost constant in a large-frequency interval (from 88 to 33 cm^{-1}), not revealing any strong decaying channel in this region. Yet near P_c (or T_c) γ increases rapidly.

Silverman[16] addressed the question of the behavior of γ near T_c (for the 0 Gpa, high-temperature Raman measurements). He suggested that the damping anomaly in $PbTiO_3$ near T_c is a frequency-dependent effect due to the

tunning of a difference combination [see Eq. (10)] of zone-boundary acoustic phonons, i.e., TO→LA-TA. His approach is based on room-temperature neutron results.[17] This point of view was also adopted by Heiman *et al.*[11] to interpret the room-temperature polariton results, which we have already discussed previously.[4] It might be possible that the zone-edge LA-TA combination, suggested by Heiman *et al.*[11] to explain their results, also decreases the required amount under pressure. An approximately 30-cm^{-1} shift would be required, which is very large for zone-edge phonons. Moreover, the data of Perry *et al.*[18] in $KTaO_3$ suggest an increase of LA-TA splitting with increasing pressure rather than a decrease.

Divergent damping behavior of γ near T_c or P_c has already been observed in other ferroelectric crystals.[19–23] Neutron and Raman measurement of the damping near the phase transition gave contradictory results when the soft phonon was overdamped.[24] In our measurements as well as in the work of Uwe and Sakudo[21,22] we observe the damping anomaly where a defined peak is observed in the spectra. Also, Uwe and Sakudo[21,22] observe this effect at 2 K, where the TA mode is not populated so that strong anharmonic decaying is unlikely. Thus, the occurrence of special resonances always near the phase transition would be highly fortuitous. From the theoretical point of view the problem remains still unsolved. Pytte,[25] using a model Hamiltonian, finds that the damping constant should be nonsingular at the phase transition for a three-dimensional system.

D. γ of $BaTiO_3$

The ferroelectric tetragonal phase of $BaTiO_3$ has the same structure and symmetry as that of $PbTiO_3$. However, while the A_1(1TO) mode is underdamped, the soft E(1TO) mode is highly overdamped. It has been suggested[11] that this has nothing to do with $BaTiO_3$ itself. Rather it occurs because the mode frequency has a value where, in perovskite crystal structures, the damping is very large (i.e., the lifetime is very short). The basis for this suggestion is the polariton measurement[11] of $\gamma(\omega)$ in $PbTiO_3$, which, as we have said, seem to contradict to our rather straightforward measurements of $\gamma(\omega)$. Rather, in $BaTiO_3$ there seems to be some intrinsic effects that produce the observed mode damping.[26] This point of view is supported by the recent hyper-Raman work of Vogt *et al.*[27] who find that at $T=430\,°C$ $\omega_0=92$ cm^{-1} yet the damping ($=280$ cm^{-1}) is still very large. This point of view is also supported by measurements on single crystals of $(Pb_{0.22}Ba_{0.78})$ TiO_3 as a function of temperature[28] and pressure.[29] In both cases, although the composition is close to pure $BaTiO_3$, the E(1TO) mode is *underdamped* except near T_c or P_c.

E. Tricritical point

We found, as was discussed above, that the phase transition at room temperature and $P_c=12.1$ GPa is second order. At atmospheric pressure and $T_c=492\,°C$ the phase transition is strongly first order.[3] Thus, our results show the existence of a tricritical point (where the phase transition changes from first to second order) in the (P,T) phase diagram of $PbTiO_3$. The existence of tricritical point in the (P,T) diagram of $PbTiO_3$ and $BaTiO_3$ was suggested by Samara[9] because the difference T_c-T_0 between the transition temperature T_c and the Curie-Weiss temperature T_0 tends toward zero with increasing pressure. A tricritical point in the (P,T) diagram was found experimentally in SbSI (Ref. 30) using Raman scattering, and in KH_2PO_4 (Ref. 31) by means of static dielectric measurements.

ACKNOWLEDGMENTS

The authors wish to thank H. Vogt and M. Cardona for helpful discussions. The technical assistance of W. Dieterich, I. Stoll, P. Wurster, H. Hirt, and M. Siemers is gratefully acknowledged. One of us (E.L.C). acknowledges the financial support of Consejo Nacional de Ciencia y Tecnología (México).

*Permanent address: Instituto de Física "Gleb Wataghin," Universidade Estadual de Campinas, 13100 Campinas, São Paulo, Brazil.

†Permanent address: Departamento de Física, Instituto de Ciencias, Universidad Autónoma de Puebla, Apartado J-48, Caixa Postal 72570 Puebla, Puebla, Mexico.

[1]G. A. Samara, T. Sakudo, and K. Yoshimitsu, Phys. Rev. Lett. 35, 1767 (1975).

[2]G. A. Samara and P. S. Peercy, in *Solid State Physics,* edited by H. Ehrenreich, F. Seitz, and D. Turnbull (Academic, New York, 1981), Vol. 36, p. 2.

[3]G. Burns and B. A. Scott, Phys. Rev. Lett. 25, 167 (1970); Phys. Rev. B 7, 3088 (1973).

[4]J. A. Sanjurjo, E. López-Cruz, and G. Burns, Solid State Commun. 48, 221 (1983).

[5]K. Syassen and W. Holzapfel, Phys. Rev. B 18, 5826 (1978).

[6]I. Fujushiro, G. J. Piermarini, S. Block, and R. G. Munro, in *High Pressure in Research and Industry,* Proceedings of the 8th AIRAPT Conference, Uppsala, edited by C. M. Backman, T. Johannison, and L. Tegner, Vol. II, p. 608.

[7]J. D. Barnett, S. Block, and G. J. Piermarini, Rev. Sci. Instrum. 44, 1 (1973).

[8]F. Cerdeira, W. B. Holzapfel, and D. Bäuerle, Phys. Rev. B 11, 1188 (1975).

[9]G. A. Samara, Ferroelectrics 2, 277 (1971).

[10]M. E. Lines and A. M. Glass, *Principles and Applications of Ferroelectric and Related Materials* (Clarendon, Oxford, 1977).

[11]D. Heiman, S. Ushioda, and J. P. Remeika, Phys. Rev. Lett. 34, 886 (1975); D. Heiman and S. Ushioda, Phys. Rev. B 17, 3616 (1975).

[12]W. Cochran and R. A. Cowley, in *Handbuch der Physik,* edited by S. Flügge and L. Genzel (Springer, Berlin, 1967), Vol. 25/2a.

[13]B. A. Weinstein, Solid State Commun. 20, 899 (1976).
[14]D. Olego and M. Cardona, Phys. Rev. B 25, 1151 (1982).
[15]S. Ushioda and J. D. McMullen, Solid State Commun. 11, 299 (1972).
[16]B. D. Silverman, Solid State Commun. 10, 311 (1972).
[17]C. Shirane, J. D. Axe, J. Harada, and J. P. Remeika, Phys. Rev. B 2, 155 (1970).
[18]C. Perry (private communication).
[19]K. Gesi, J. D. Axe, and G. Shirane, Phys. Rev. B 5, 1933 (1972), but these results were later criticized by S. M. Shapiro, J. D. Axe, G. Shirane, and T. Riste, *ibid.* 6, 4332 (1972).
[20]D. J. Lockwood and B. H. Torrie, J. Phys. C 7, 2729 (1974).
[21]H. Uwe and T. Sakudo, Phys. Rev. B 13, 271 (1976).
[22]H. Uwe and T. Sakudo, Phys. Rev. B 15, 337 (1977).
[23]T. Inushima, K. Uchinokura, K. Sasahara, and E. Matsuura, Phys. Rev. B 26, 2525 (1982).
[24]S. Satija and R. A. Cowley, Phys. Rev. B 25, 6765 (1982).
[25]E. Pytte, Phys. Rev. B 1, 924 (1970).
[26]G. Burns and B. A. Scott, Solid State Commun. 9, 813 (1971).
[27]H. Vogt, J. A. Sanjurjo, and G. Rossbroich, Phys. Rev. B 26, 5904 (1982).
[28]G. Burns (unpublished).
[29]J. A. Sanjurjo, E. López-Cruz, and G. Burns (unpublished).
[30]P. S. Peercy, Phys. Rev. Lett. 35, 1581 (1975).
[31]V. H. Schmidt, A. B. Western, and A. G. Baker, Phys. Rev. Lett. 37, 839 (1976).